Flow-Accelerated Corrosion Behavior of A106 Gr.B in Simulated PWR Secondary Water with Different pH and pH Control Agents

Jeoh Han [a,b], Soon-Hyeok Jeon [a], Hee-Sang Shim [a], Young-Kook Lee [b], Do Haeng Hur [a,*]
[a]*Korea Atomic Energy Research Institute, Materials Safety Technology Research Division, Daejeon, 34057, Republic of Korea*
[b]*Yonsei University, Department of Materials Science and Engineering, Seoul, 03722, Republic of Korea*
[*]*Corresponding author: dhhur@kaeri.re.kr*

1. Introduction

Flow-accelerated corrosion (FAC) is one of the typical material degradation model that shortens pipeline life in fossil-fuel plants and nuclear power plants [1]. Since the FAC is mainly generated in the secondary coolant system of pressurized water reactors, water chemistry of the secondary water is strictly managed in an alkalized reducing condition to mitigate the FAC phenomenon. In this regard, the pH of the secondary water is maintained in the range of 9.0 to 10.0 at 25 ℃, and ethanolamine (ETA) and ammonia (NH_3) are used as pH control agents [2]. Unfortunately, even above water chemistry conditions can not completely prevent the FAC phenomenon of carbon steel piping [3]. This is because the oxide film formed on the inner surface of the pipe has still poor protective characteristics, thereby leading to dissolution. Although there are many studies on the effects of pH control on the FAC of carbon steel materials in secondary water [4, 5], most of the FAC behavior was investigated in terms of weight or thickness change.

In this study, the effects of two different pH (9.0 and 10.0 at 25 ℃) and pH control agents (ETA and NH_3) on the FAC behavior were investigated together in terms of oxide film characteristics as well as weight change. Furthermore, electrochemical properties of oxide films formed during FAC tests were investigated.

2. Experimental Methods

2.1 FAC tests

Specimens for FAC and electrochemical tests were fabricated from an A106 Gr.B pipe. Each FAC test was conducted using a circulation loop system of single-phase water at 150 ℃ and 500 h. The test solution was prepared to have a pH value of 9.0 or 10.0 at 25 ℃ by adding each pH control agent in the deionized water. Dissolved oxygen concentration was maintained below 5 ppb by blowing N_2 gas. When the temperature of the solution was stabilized at 150 ℃, specimens were rotated so that the linear velocity at the surface of specimens was 5 m/s until the end of the test. The corrosion rates of the specimens were calculated using the weight changes of the specimens before and after the test.

2.2 Characterization of oxide films

The surfaces of oxide films were observed using scanning electron microscopy (SEM). The cross-sections of the oxide films were observed using SEM after milling using the focused-ion beam (FIB). The chemical compositions of the oxide films were analyzed using energy dispersive spectroscopy (EDS) attached to a transmission electron microscope (TEM).

2.3 Electrochemical tests

Electrochemical properties of oxide films formed during the FAC tests were investigated through Mott-Schottky plots at 25 ℃. A borated buffer solution (0.05 M H_3BO_3 + 0.075 M $Na_2B_4O_7$) was used as the test solution. After the open-circuit potential was stabilized, capacitance values were measured at a frequency of 1000 Hz in the potential range of + 1.5 to - 1.0 V. An AC signal with a 10 mV amplitude was applied to the cell.

3. Results and Discussion

Fig. 1 shows the corrosion rates of A106 Gr.B specimens after each FAC test.

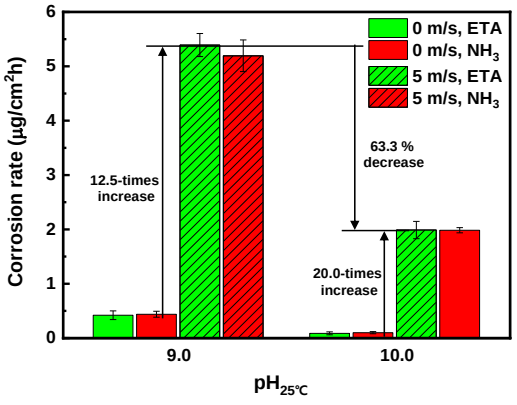

Fig. 1. Corrosion rate of the A106 Gr.B specimens after the FAC tests.

The corrosion rates increased by 12.5-times and 20.0-times, respectively, in the $pH_{25℃}$ 9.0 and 10.0 solution when the fluid velocity increased from 0 to 5 m/s. At the same fluid velocity of 5 m/s, the corrosion rate

decreased by 63.3 % in the $pH_{25℃}$ 10.0 solution than in the $pH_{25℃}$ 9.0 solution. On the other hand, the significant difference of the corrosion rates was not observed according to the pH control agents. This means that the FAC resistance of A106 Gr.B is more dependent on the pH than the pH control agents.

Fig. 2 shows the surface and cross-section SEM images after the FAC tests in the $pH_{25℃}$ 9.0 and 10.0 solution adjusted with NH_3. In the $pH_{25℃}$ 9.0 solution, the oxide particles formed on the surface were extremely small with a size of several tens of nanometers, and thickness of the oxide film was about 1.7 μm. However, the oxide particles formed in the condition of $pH_{25℃}$ 10.0 were clearly observed to have a large polyhedral-shape of about 0.5 μm, and thickness of the oxide film was about 1.2 μm. The oxide films formed in both different pH solution had many pores. However, the oxide film formed in $pH_{25℃}$ 10 solution was denser on the side adjacent to the matrix. This means that the dissolution rate of oxide film reduced at the higher pH, resulting in the he lower corrosion rate.

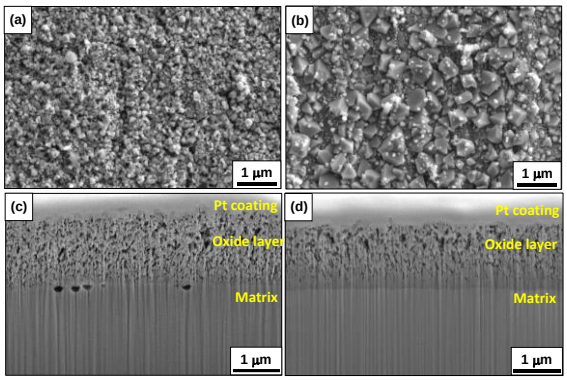

Fig. 2. SEM images of the surfaces and cross-sections of the oxide films in different pH conditions adjusted with NH_3: (a) and (c) $pH_{25℃}$ 9.0, (b) and (d) $pH_{25℃}$ 10.0.

Fig. 3 shows the Mott-Schottky plots of oxide films formed under different pH and pH control agents during FAC tests. The capacitance values of oxide films formed in the $pH_{25℃}$ 10 solution was smaller than those in the $pH_{25℃}$ 9.0 solution in the range of - 0.2 V to 0.8 V, regardless of the pH control agents. The capacitance responses of oxide films showed the positive slope in region I and negative slope in region II, indicating an n-type and a p-type semiconductor behavior, respectively.

The total point defect densities of oxide films were calculated as shown in Table I through the linear slope of the Mott-Schottky plots. The total point defect densities were similar regardless of pH control agents under the same pH conditions. However, it was decreased by 26 % under the $pH_{25℃}$ 10.0 condition than that under the $pH_{25℃}$ 9.0 condition. Since a point defect can act as a migration path for metal cations or oxygen ions, oxide film formed in the high pH solution is more resistance to the FAC. These results are in good agreement with the corrosion rates and morphologies of the oxide film.

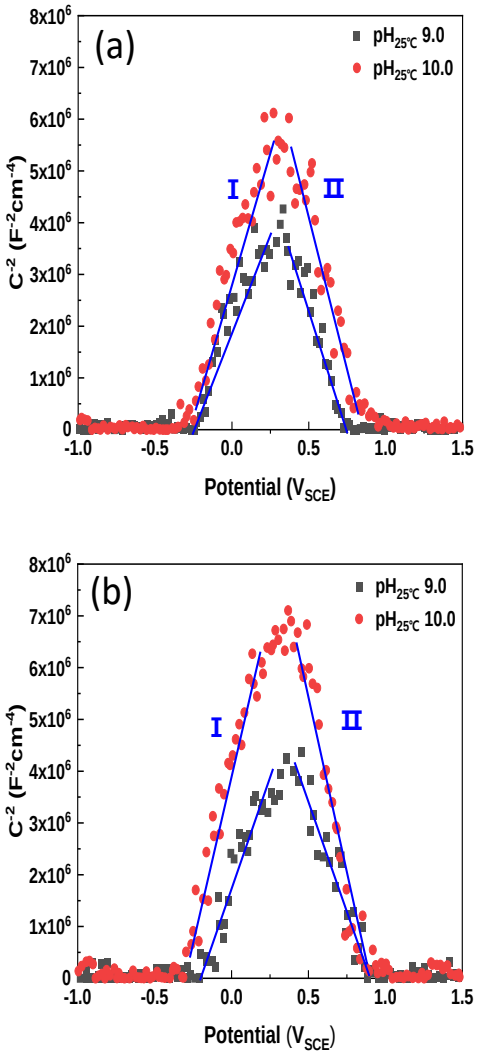

Fig. 3. Mott-Schottky plots of oxide films after the FAC tests: (a) ETA solution, (b) NH_3 solution.

Table I: Total point defect densities of oxide films

pH control agent	$pH_{25℃}$	Total point defect density (cm^{-3})
ETA	9.0	1.68×10^{24}
	10.0	1.25×10^{24}
NH_3	9.0	1.53×10^{24}
	10.0	1.11×10^{24}

4. Conclusions

The FAC behavior of A106 Gr.B material was investigated under different pH and pH control agent conditions, and the obtained conclusions were as follows.

(1) The corrosion rates by FAC decreased by 63.3 % when the $pH_{25°C}$ increased from 9.0 to 10.0 at a fluid velocity of 5 m/s. However, the difference between two types of pH control agents were not meaningful influenced on the FAC rates of A106 Gr.B.
(2) The size of oxide particles was larger when the $pH_{25°C}$ of the solution was 10.0 than 9.0. The oxide films formed in the NH_3 solution were porous regardless of the pH value. However, the thickness of the oxide film was thinner when it was formed in the $pH_{25°C}$ 10 solution, and the side adjacent to the matrix was more dense.
(3) The point defect densities of the oxide films decreased when formed under the high pH solution. On the other hand, the point defect densities of oxide films were insensitive to the change of the pH control agents of the secondary water.

ACKNOWLEDGEMENTS

This work was supported by the National Research Foundation (NRF) grant funded by the government of the Republic of Korea (grant number: NRF-2018M2A8A4081307, RS-2022-00143316).

REFERENCES

[1] V. Kain, Flow Accelerated Corrosion: Forms, Mechanisms and Case Studies, Procedia Eng. 86, 576-588, 2014.
[2] K. Fruzzetti, Pressurized Water Reactor Secondary Water Chemistry Guidelines-Revision 8, EPRI, 3002010645, 2017.
[3] B. Poulson, Predicting and Preventing Flow Accelerated Corrosion in Nuclear Power Plant, Int. J. Nucl. Energy, 1-23, 2014.
[4] J.L. Singh, U. Kumar, N. Kumawat, S. Kumar, V. Kain, S. Anantharaman, and A.K. Sinha, Flow Accelerated Corrosion of Carbon Steel Feeder Pipes from Pressurized Heavy Water Reactors, J. Nucl. Mater. 429, 226-232, 2012.
[5] H.P. Rani, T. Divya, R.R. Sahaya, V. Kain, D.K. Barua, CFD Study of Flow Accelerated Corrosion in 3D Elbows, Ann. Nucl. Eng. 69, 344-351, 2014.